ELSEVIER

PII: S0032-3861(97)00321-2

Polymer Vol. 39 No. 3, pp. 591–597, 1998

0032-3861/97/$17.00+0.00

Polymerisation process of 1,6-di(*N*-carbazolyl)-2,4-hexadiyne epitaxially grown films studied by high-resolution electron microscopy

Noboru Kawase[a], Seiji Isoda[b,*], Hiroki Kurata[b], Yukio Murata[a], Kenji Takeda[c] and Takashi Kobayashi[b]

[a]*TORAY Research Center, Sonoyama, Otsu, Shiga 520, Japan*
[b]*Institute for Chemical Research, Kyoto University, Uji, Kyoto 611, Japan*
[c]*Japan Synthetic Rubber, Miyukigaoka, Tsukuba, Ibaraki 305, Japan*
(Received 15 November 1996; revised 28 February 1997)

Thin films of 1,6-di(*N*-carbazolyl)-2,4-hexadiyne (DCHD) grown epitaxially on (0 0 1) surface of KCl through vacuum-deposition were examined on their polymerisation process induced by heat treatment or electron irradiation. The structural changes due to polymerisation in the films were investigated by electron diffraction and low temperature high resolution electron microscopy. By electron irradiation, many small crystallites of polymer were produced randomly in the monomer single crystal keeping the topochemical relation. The nucleation of polymer crystals is considered to be 'homogeneous' in this case. In contrast, thermal polymerisation resulted in bigger fibrous polymer crystals with the same topochemical relation, but different orientations were also observed at the edges of the crystal, which means that the polymerisation is 'heterogeneous'. High-resolution images of partially polymerised specimens by heat treatment showed small grains of transient states with intermediate lattice spacings between monomer and polymer crystals. Therefore, the polymerisation of DCHD proceeds through the transient stage of crystal structure without definite phase separation of monomer and polymer in the case of thermal polymerisation. In addition to this, the polymer crystals were found to be formed first at the edges of monomer crystals, and thereafter may change their orientation so as to relax an inner stress produced by further polymerisation at the inner part of monomer crystals. © 1997 Elsevier Science Ltd.

(Keywords: 1,6-di(*N*-dicarbazolyl)-2,4-hexadiyne; polymerisation process; low temperature high resolution imaging)

INTRODUCTION

Since Wegner demonstrated in 1969 that solid-state polymerisation of diacetylenes can be characterised as a diffusionless and lattice controlled process[1], many solid-state reactions in diacetylene derivatives have been examined on their unique features[2–5]. These polymerisation reactions are caused by specific rotations of the monomers followed by 1,4-addition of adjacent units as shown in *Figure 1*. The polymerisation process of these monomer crystals is of special importance, because the quality of the resulting polymer single crystal governs well-known properties in optical nonlinearity. Since such macroscopic optical properties of the materials depend not only on their molecular characteristics but also on their state of aggregation, it is important to characterise their microscopic polymerisation process in detail.

With respect to 1,6-di(*N*-carbazolyl)-2,4-hexadiyne (DCHD), Enkelmann *et al.*[6] reported in 1977 that DCHD monomer crystals can be topochemically polymerised by heat treatment or γ-irradiation. They analysed the crystal structures of the monomer and the polymer crystals by X-ray. In addition, the conversion-dependent phase transition has been reported, which indicates the existence of solid-solution of monomeric and polymeric molecules. More recently, structure investigations of the polymer have been carried out by direct imaging with a high-resolution electron microscope (HREM)[7,8]. Concerning monomer and partially polymerised crystals, however, such direct imaging is very difficult, because the DCHD monomer is easily polymerised even under weak electron irradiation, in addition to the fact that the crystal is quickly damaged.

Since HREM can directly reveal the molecular arrangement and local states of aggregation, there are several studies employing the direct imaging method with HREM on polymers[9–12]. However, only few works have studied the polymerisation process. In our previous study on a polymerisation process with HREM[13], solid-state polymerisation of silicon phthalocyanine deposited epitaxially on mica substrate was investigated in detail during its thermal polymerisation, in which the polymerisation sites and the polymerisation process were revealed by HREM. For the polymerisation of DCHD, Liao and Martin have tried to record HREM images dynamically on video tape under a very weak electron dose of 10^{-4} C cm^{-2} as well as electron diffraction patterns[14]. They succeeded in observing 1.2 nm lattice fringes (the (010)-plane of the polymer crystal) during electron irradiation. However, they did not report either shorter lattice fringes of polymer or lattice fringes of monomer crystal, probably due to a low S/N ratio under such a weak electron dose.

In the present study, the high resolution work was performed by cooling the specimen at a low temperature with a cryo specimen holder and employing a minimum electron irradiation system for image recording, as

* To whom correspondence should be addressed. Tel.: 81+(0)774-38-3051; fax: 81+(0)774-33-7096

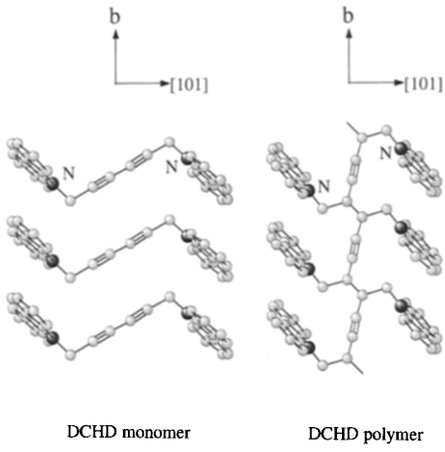

Figure 1 DCHD monomer and polymer obtained by γ-irradiation or thermally induced 1,4-addition reaction. The b-axis is the common axis in topochemical reaction, which is the chain direction of DCHD polymer

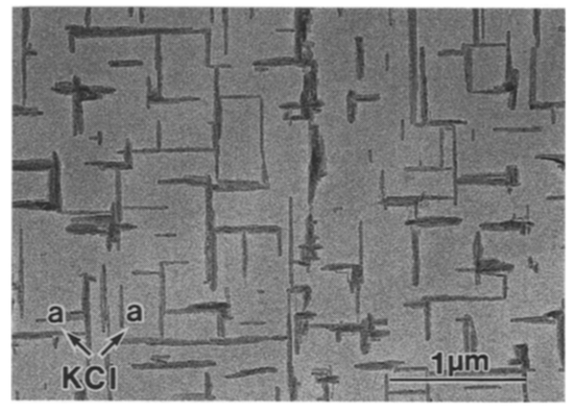

Figure 2 DCHD film grown epitaxially on KCl. Needle-like crystals orient their longer axis (b-axis) along the [1 1 0] or [1 $\bar{1}$ 0] direction on the KCl surface

described later in detail. The structural correlation of thin poly-DCHD film with the monomer film grown epitaxially on a substrate are examined by high resolution imaging to elucidate the polymerisation process. The partially polymerised stages as well as the monomer and the polymer crystals were observed with cryo-HREM.

EXPERIMENTAL

Preparation of epitaxial films of DCHD

A small amount of the DCHD powder was heated in a quartz crucible wound with a molybdenum wire-heater in the vacuum of 5×10^{-5} Pa, and the sublimed material was condensed as a thin film on a single crystalline substrate. Because prolonged heating of DCHD in the crucible was found to induce thermal polymerisation in the crucible, the sublimation was done by flash-heating. Film thickness was monitored by a quartz oscillator microbalance and kept at less than 15 nm. The (0 0 1) surface of freshly cleaved alkali-halide single crystals or mica was used as the substrate. Several pieces of single crystalline substrates, $10 \times 10 \times 1$ mm^3 in size, were mounted on a hot plate and pre-heated at about 400°C for 2 h in vacuum of 5×10^{-5} Pa to eliminate surface contaminants of substrate. The temperature was then lowered to and maintained at 50°C during deposition. The substrate temperature is important for obtaining an epitaxial film of monomeric DCHD, because above 90°C the material was polymerised immediately on substrate.

Polymerisation of epitaxial monomer films

The polymerisation of DCHD was carried out by two methods. The first method is polymerisation by heating; the epitaxial films on the substrate were heated to 150°C in a nitrogen atmosphere. The second method is electron irradiation at 20°C in a vacuum of 10^{-4} Pa in a transmission electron microscope (TEM) at an accelerating voltage of 200 kV, where a very low electron dose of 10^{-4} C cm^{-2} is enough to polymerise the monomer crystals as reported[14]. At this amount of dosage, the specimen suffers almost no radiation damage.

Electron microscopy

Since the deposited monomer DCHD film was very easily polymerised by weak electron irradiation at room temperature, electron microscopic observation of the monomer crystals had to be carried out at low temperatures. Below −50°C, the monomer does not polymerise even under an electron dose of 10^{-1} C cm^{-2}, but a degradation in crystallinity of basic monomeric structure was observed depending on dosage. A cryo specimen holder (Oxford UHRST-3500) was used to keep the specimen at a low temperature, between −50 and −110°C, in a JEM2000FX electron microscope having a theoretical point-to-point resolution of 0.35 nm. The monomer and the partially polymerised specimens were observed at these temperatures. The fully polymerised specimens were observed at room temperature, because no further polymerisation was expected. In this case, high resolution images were taken with a JEM 200CX electron microscope (theoretical resolution 0.2 nm). Both microscopes were operated at 200 kV and were equipped with a minimum-dose irradiation system (MDS)[15], which avoids unnecessary electron irradiation damage before taking an electron micrograph. For extra strength the specimen was coated with a thin carbon film (~3 nm), and was then fixed on electron microscopic grids after floating the substrate off on water. Optical absorption of the films was measured with a UV-Vis spectrometer, Shimadzu UV-2200, to check the extent of polymerisation[16].

RESULTS AND DISCUSSION

Orientation of epitaxially grown DCHD

A typical electron micrograph of DCHD monomer grown on the (0 0 1) of KCl is shown in *Figure 2*. The film is composed of many needle-like crystals with their longer axis along the two directions of [1 1 0] and [1 $\bar{1}$ 0] of the substrate KCl. The width of each needle-like crystal is several tens of nanometers and the length reaches about 1 μm. The needle axis corresponds to the b-axis of DCHD monomer crystal as revealed by selected-area electron diffraction (SAED). As the amount of deposited DCHD is increased, these needle-like crystals increase their size and finally the deposited film becomes continuous. Our TEM observation was carried out on the needle-like crystals because observation at the edges of crystals was believed to be important in order to analyse the polymerisation process, particularly to determine the initial polymerisation sites. The optical absorption measurement was performed for the deposited monomer film. The absorption peak located at

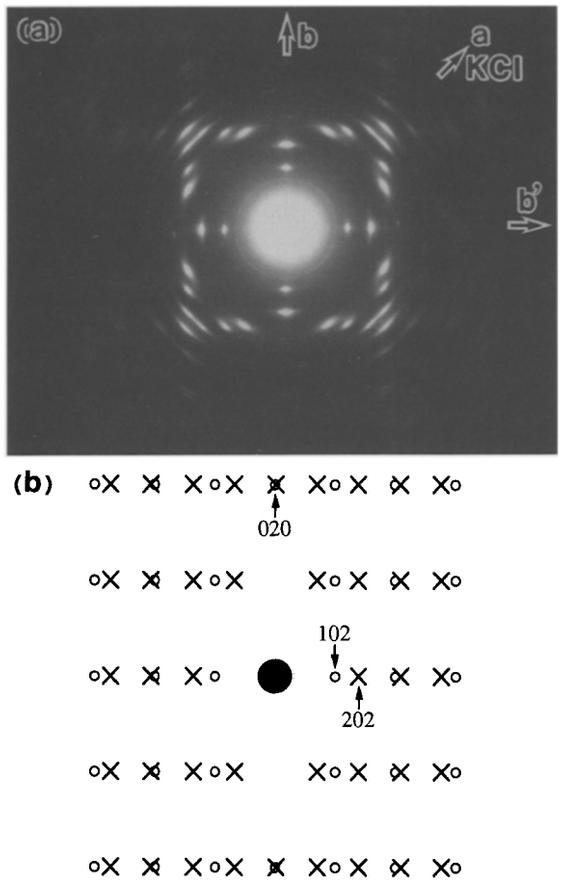

Figure 3 (a) SAED pattern of epitaxially grown monomer crystals corresponding to Fig. 2. Two sets of diffraction pattern are overlapped with 90°. (b) Schematic illustration of one of the overlapping patterns observed in (a)

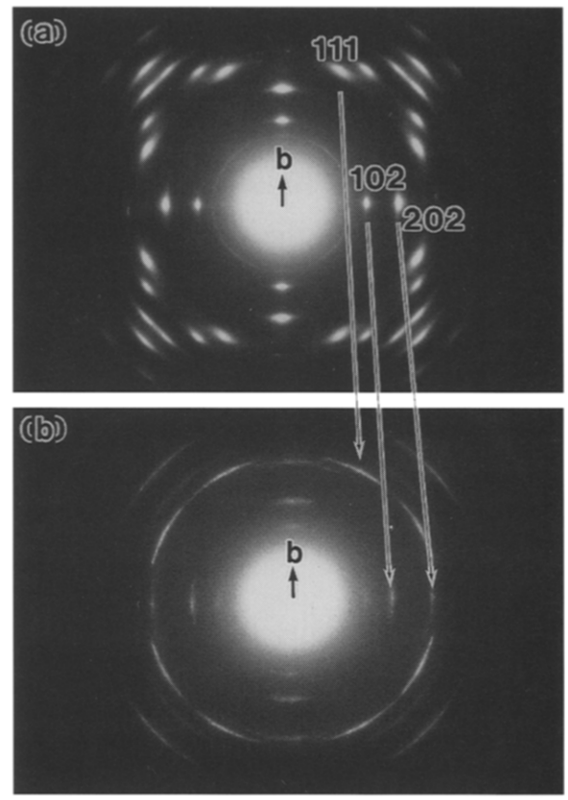

Figure 4 Electron diffraction patterns from (a) DCHD monomer and (b) poly-DCHD polymerised by electron-beam

655 nm, which is known to increase in intensity with the polymerisation[16], was not observed. Accordingly, it can be concluded that polymerisation did not occur in the deposited crystallites during the vacuum-deposition process.

The corresponding SAED pattern of the monomer epitaxial crystal is shown in *Figure 3a*, this was taken from an area of 0.5 μm diameter in *Figure 2*. The DCHD monomer has been reported to have the following lattice constants[6]; $a = 1.36$ nm, $b = 0.455$ nm, $c = 1.76$ nm and $\beta = 94°$ in the monoclinic unit cell of $P2_1/c$. In the diffraction, two sets of pattern are superimposed at a right angle. One of the superimposed patterns is represented schematically in *Figure 3b*, which clearly demonstrates that the monomer crystal grows making its b-axis, i.e. needle axis, parallel to the [1 1 0] or [1 $\bar{1}$ 0] axis of the substrate KCl and its (1 0 $\bar{1}$) and (2 0 $\bar{1}$) plane nearly parallel to the (001) surface of the substrate. The other set of such diffraction is superimposed on the first one, rotated with an angle of 90°, so that it is eventually interpreted that the crystals grow in two equivalent orientations relative to the [1 1 0] of substrate lattice. Almost the same epitaxial films have been observed on KBr substrate by Moigne *et al.*[17]. In the present study, single crystals of KBr, NaCl and mica were also used as the substrate. The epitaxial orientation of each deposition film was determined as follows. On KBr, the same kind of orientation was observed as on KCl, but the diffraction spots are not so sharp as on KCl. On NaCl, diffraction patterns with four orientations were found; that is, the b-axis of the monomer crystal orients along the [1 1 0], [1 $\bar{1}$ 0], [1 0 0] or [0 1 0] of NaCl. As opposed to these substrates, random orientation of monomer crystals was observed on mica. For further investigation, KCl was used as the substrate, because the epitaxial orientation on KCl is preferable for high resolution observation.

Polymerisation process

Electron diffraction pattern of the thin film on KCl (*Figure 4a*) was changed by electron-induced polymerisation as shown in *Figure 4b*. This latter pattern corresponds to those of poly-DCHD crystals reported by Apgar[18]. He has analysed the DCHD polymer structure with the following monoclinic lattice constants: $a = 1.28$ nm, $b = 0.491$ nm, $c = 1.74$ nm and $\beta = 108.3°$, and belongs also to the space group of $P2_1/c$. The diffraction pattern in *Figure 4b* can be indexed using these lattice constants. The corresponding diffraction spots in monomer and polymer are linked by arrows in the figures. It is known that bulk crystal of DCHD monomer is polymerised through topochemical solid-state reaction[4,16]. In the thin film, the b-axis (the chain) direction of the polymer crystals remains unchanged from that of the monomer, and the other reflections of polymers are observed to coincide with the corresponding reflections in the monomer. Therefore, the polymerisation reaction in thin film is also a topochemical solid-state reaction as a whole, although some distortion and disorder in orientation are introduced during polymerisation, as discussed later.

HREM is a powerful method for the study of the polymerisation process at the microscopic scale, but it is very hard in general to take high resolution images of organic crystals, owing to severe radiation damages. In addition to this radiation damage, the monomer crystals of DCHD polymerise easily under weak electron irradiation

(about 10^{-4} C cm^{-2}) at room temperature, which makes the matter worse. However, when electron microscopic observation of monomer crystals was carried out at temperatures lower than -50°C, it was found that polymerisation had not taken place. Thus, the cryo specimen holder in the electron microscope was necessary for the present study. At this low temperature, the thermal motion of the monomer is depressed such that polymerisation is not induced, even under higher electron radiation of 10^{-1} C cm^{-2}, which allows an image to be recorded at a magnification of 50 000. With lowering of the temperature, the lattice parameters are decreased by about 1% in the b-axis direction at -150°C compared with that at room temperature. Such shrinkage of lattice spacing is unfavourable for the polymerisation of DCHD[3], and this may be an additional factor suppressing polymerisation at low temperature. At -131°C, DCHD monomer is known to undergo a first order phase transition into an unreactive low temperature crystal phase[19], which is accompanied by a large decrease in the b-axis length of about 8%. However, the thin film used in the present study did not change into the low temperature phase even at -170°C, and kept its high temperature structure. This may be a thin film characteristic, but it is as yet unclear why the epitaxial films do not transform into the low temperature phase. However, high resolution imaging of the monomer or partially polymerised DCHD can be performed with the aid of cryo electron microscopy and MDS.

Figure 5a and *c* show high resolution images of monomer crystal observed at -100°C and of polymer crystal at room temperature, respectively. Both images are the projections along the [1 0 $\bar{1}$] axis of the respective crystals. *Figure 5b* and *d* are the computer-simulated images for the corresponding crystals. In order to interpret intuitively a high resolution image, one must pay much attention to imaging conditions, especially to specimen thickness and defocus value. As the specimen in the present work is thin (about 15 nm) and contains no heavy atoms, the dynamical effect of electrons in the specimen could be negligible. In both images in *Figure 5*, the (202) lattice fringes can be observed clearly with the spacing of 0.52 nm for monomer and 0.43 nm for polymer, and furthermore a herring-bone structure corresponding to carbazolyl group can also be recognised in the polymer image. These images prove that the monomer and the polymer regions can be discriminated in such a high resolution image of partially polymerised crystals.

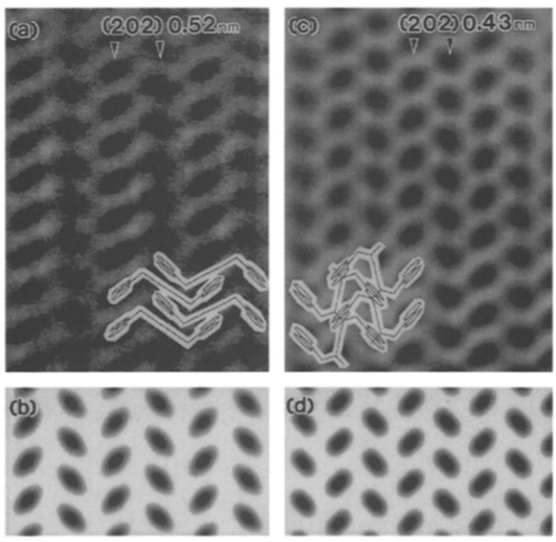

Figure 5 (a) High resolution image of monomer crystal obtained as a projection along the [1 0 $\bar{1}$] axis. (c) High resolution image of polymer crystal obtained as a projection along the [1 0 $\bar{1}$] axis. (b) and (d) show corresponding images simulated from the molecular packings for both crystals

Differences in crystallinity and orientations caused by different polymerisation methods (heating or electron irradiation) are shown in electron diffraction patterns of *Figure 6*, in which *a* and *b* are the SAED patterns of polymer crystals polymerised fully by heating at 150°C for 5 h and by electron irradiation of 10^{-4} C cm^{-2} at 20°C in electron microscope, respectively. Both diffraction patterns were taken from the selected area of 0.2 μm in diameter. The electron-induced polymer exhibits arc-like SAED, which indicates that the monomer crystals are divided into many small polymer crystallites whose orientations have fluctuated slightly from the exact topochemical orientation with respect to the mother monomer crystal. In contrast to this, the crystals polymerised by heat treatment give spotty reflections, which means that a limited number of polymer crystallites contribute the electron diffraction spots.

To reveal the microscopic features of such polymer crystals, high resolution imaging was employed. A high resolution image of polymer crystal obtained by heating a monomer film on the KCl substrate at 150°C for 5 h is shown in *Figure 7a*. The optical absorption spectrum of this film exhibits an absorption peak at 655 nm, whose intensity did not increase by further heating. Therefore, the polymerisation reaction has been completed. The high resolution image shows a part of a needle-like crystal, including an edge which is indicated by the two larger black arrows inserted in the image. The vertical direction of the figure is the needle axis, i.e. b-axis of the polymer. At inner part of the crystal (the right part of the image), lattice fringes of 0.43 nm are observed along two directions developing over a large area. The angle between these lattice fringes is about 59° and the angle of the fringe with the b-axis is about 60°, which agrees well with values calculated from the polymer crystal, assuming that the lattice fringes come from the (1 1 1)- and (1 $\bar{1}$ 1)-planes. The area, therefore, can be assigned as a projection of polymer crystal along the [1 0 $\bar{1}$]. *Figure 7b* illustrates schematically the electron micrograph shown in *Figure 7a*. At the edge of the crystal, lattice fringes of 0.83 nm are running along the b-axis, which corresponds

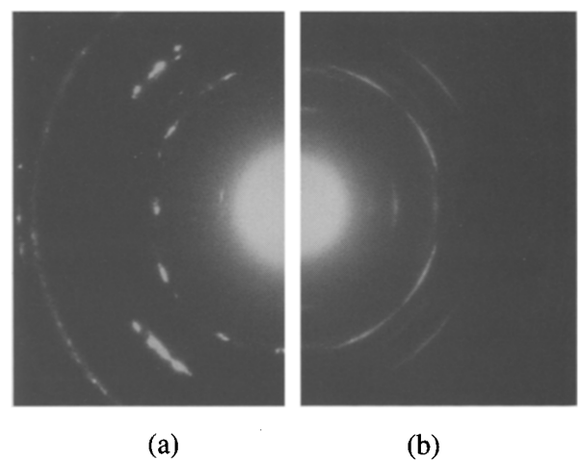

Figure 6 Electron diffraction patterns from DCHD polymerised (a) by thermal annealing at 150°C and (b) by electron irradiation at 20°C

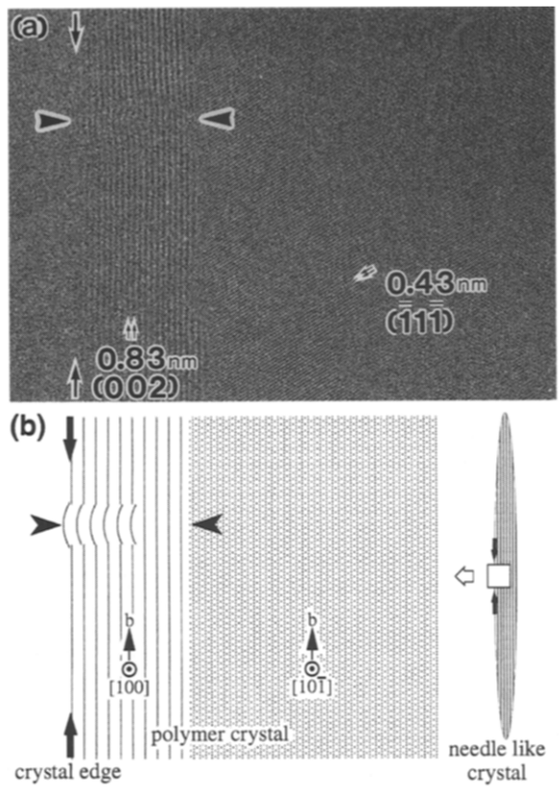

Figure 7 (a) High resolution image of fully polymerised film by thermal treatment for 5 h at 150°C, where the vertical arrows indicate the crystal edge. (b) Schematic illustration of (a). At the inner part of the needle-like crystal, polymerisation proceeds in a manner expected from topochemical reaction, but at the edge the polymerised crystal changes its orientation drastically. With thermal treatment the polymer grows longer in size along the b-axis of chain direction

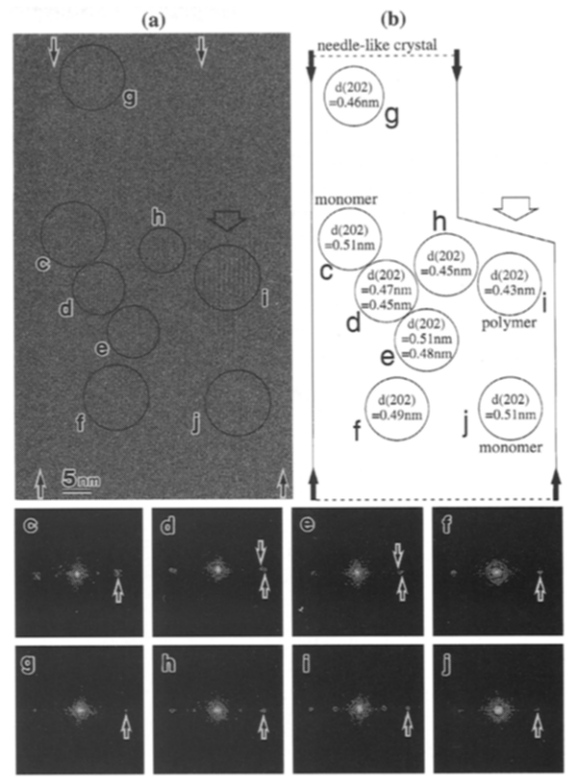

Figure 8 (a) High resolution image of partially polymerised crystal for 3 min at 150°C. (b) Schematic illustration corresponding to (a). Diffractograms shown below are Fourier transforms of the corresponding small circular regions in (a), from which lattice spacings appearing in the high resolution image can be determined locally. In the high resolution image, the polymerisation seems to start at the defect region i, where only the lattice spacing of polymer is observed. In the regions c–f and h, the solid-solution of monomer and polymer are formed as transient stages, but in the regions of c and j, no polymerisation occurs

to the spacings of (0 0 2). This lattice plane could not satisfy the Bragg condition if the polymerisation of monomer crystal occurs topochemically, as illustrated in *Figure 4*. If the poly-DCHD changes its orientation from the topochemical one by rotating about 28° around the b-axis, then the (002) lattice fringes become observable in HREM. By careful inspection on SAED, one can find weak 002-reflections in the original negatives for the thermally induced poly-DCHD. This type of change in crystal orientation was frequently observed at the edges of other crystals polymerised thermally. The poly-DCHD crystals seem to grow in many cases by changing drastically their orientation at the crystal edge, because such rotation is needed probably to relax a stress produced during polymerisation. In addition to this orientation change, crystal distortion is observed at the edges indicated by the two black arrowheads in *Figure 7a*. This distortion may be introduced by collision of two growing polymer crystals from the opposite sides along the b-axis. Thus, the DCHD molecules change their orientation, especially at the crystal edge where it is easy to expand the volume and to change orientation.

To examine the process of polymerisation, it is necessary to observe intermediate stages of the polymerisation as well as the initial and final stages. A high resolution image at such intermediate stage of polymerisation is shown in *Figure 8a* as a projection nearly along [1 0 $\bar{1}$] axis of polymer, where the vertical is the b-axis direction. This needle-like crystal is very small and the edges on both sides are shown by the four black arrows in *a*. The width of the crystal is about 50~80 nm. Polymerisation was done by heating the monomer film at 150°C for 3 min. By optical absorption measurement, it was confirmed that the polymerisation reaction has proceeded only slightly. Various lattice fringes having different spacings can be found in the crystal. *Figure 8b* summarises the lattice fringes observed in *Figure 8a*. Each lattice interval is obtained from an optical Fourier transform of respective small domains indicated by the circles in *Figure 8a*. The encircled domains are indicated from c to j. Fourier transform gives a diffractogram for each small region as shown below in the figure. The lattice spacings measured from these diffraction spots are summarised in *Figure 8b* with their Miller indices. For example, in region i the lattice fringes have a spacing of 0.43 nm, which corresponds to the (2 0 2)-spacing of the polymer. On the other hand, in regions c and j, lattice fringes have a spacing of 0.51 nm, corresponding to the (2 0 2)-spacings of the monomer. From this micrograph it becomes clear that the polymer and the monomer crystallites coexist as small domains in partially polymerised crystal. The regions of d~f and h show intermediate lattice spacings between those of the monomer and polymer, so these regions are considered to be a mixed crystal or a solid solution of monomer and polymer molecules. Since all values of lattice spacings observed in the image are between those of monomer and polymer crystals, it can be concluded that various transient states of crystal structure coexist at microscopic level in partially polymerised crystal. This result supports the previous X-ray study on bulk specimen [16], and

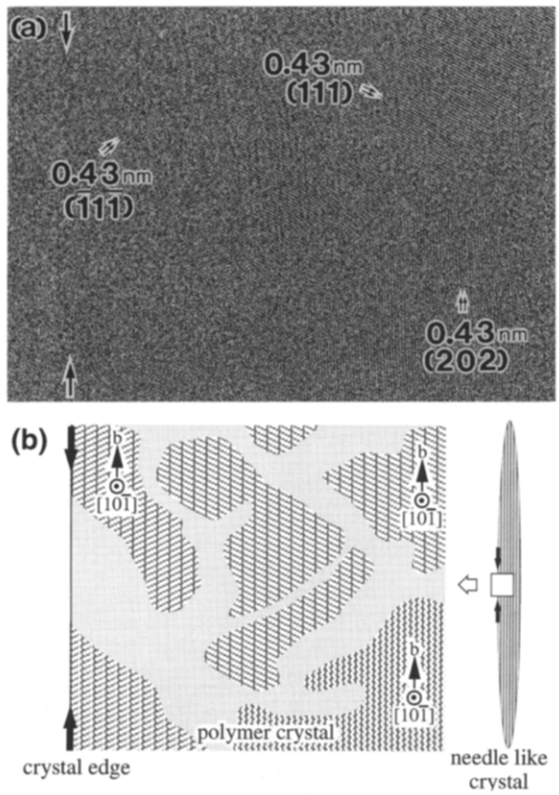

Figure 9 (a) High resolution image of fully polymerised film by electron irradiation at 20°C. The vertical large arrows indicate the edge of the needle-like crystal. (b) Schematic illustration of (a), in which the cross-hatched island regions represent the domains showing lattice fringes in (a). The single crystal of the monomer is found to be crystallised into fine polymer crystallites by electron irradiation

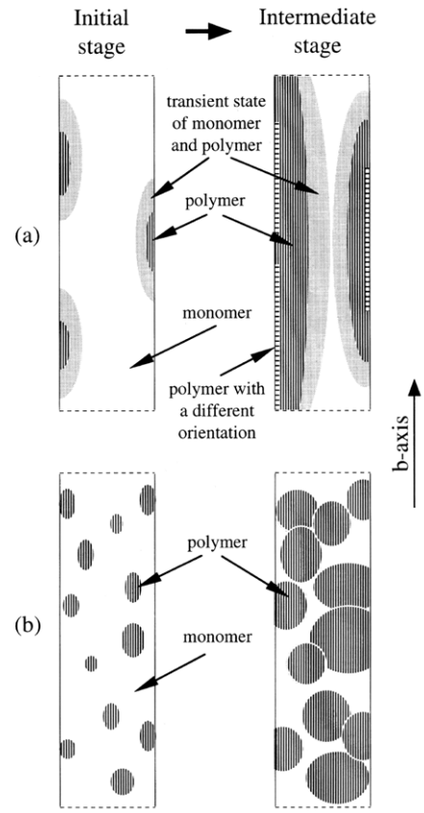

Figure 10 Anticipated polymerisation processes (a) by thermal annealing and (b) by electron irradiation are shown at the initial and the intermediate states of polymerisation for both cases. In the thermal polymerisation, the nucleation is heterogeneous preferentially at the edge, and the polymer crystals grow as fibrous texture accompanying the transient regions. On the other hand, the nucleation in the radiation-induced polymerisation is homogeneous, and the nuclei grow independently into small grains with nearly coherent relationships with each other

gives new information. That is, the transient state is an aggregation of very small crystallites having slightly different lattice spacings in needle-like crystal which was originally a single crystal of monomer. In addition to this, it is interesting that the almost polymerised region i is found at a crystal edge indicated by the wide white arrow, where the monomer crystal ended along the b-axis. On the other hand, at the inner parts of the crystal, polymerisation did not start or did not complete, as indicated by the lattice fringes with different spacings in the figure. Then the thermal polymerisation could start from such a defect at crystal edge, as in the case of silicon phthalocyanine [13]. As polymerisation proceeds the small domains of solid-solution may coalesce coherently each other along the chain axis, resulting in a large fibrous domain as observed in *Figure 7*. Finally, the large domain at the edges of needle-like crystal, considered to be a domain fully polymerised at an early stage, may change its orientation drastically, probably to relax a stress produced by polymerisation at the inner part of the crystal.

In contrast to thermal polymerisation, polymer crystal produced by electron irradiation gives a different type of high resolution image as shown in *Figure 9a*, in which the vertical has been the b-axis direction of the monomer crystal. This thin film was irradiated by electron dosage of about 10^{-4} C cm^{-2} at room temperature in electron microscope. By an optical absorption measurement, the peak at 655 nm was found to be saturated, showing that the polymerisation reaction had been completed. *Figure 9b* is a schematic illustration of the domain structures in *Figure 9a*. In both figures the large arrows indicate crystal edge of a needle-like crystal. In the crystal, lattice fringes of 0.43 nm corresponding to (1 1 1) and (2 0 2) planes are observed in many small regions, all of which can be interpreted nearly as the projection along the [1 0 $\bar{1}$] of the polymer. The (1 1 1) and the (2 0 2) planes have almost the same spacings of 0.43 nm nearly with topochemical orientations as expected from the reaction. Here again the polymer crystal grows almost topochemically, even though the orientation of the crystallites fluctuates slightly with respect to each other, as discussed before from SAED in *Figure 6b*. The most distinguishing features of the image are that (i) none of the high resolution images show large orientational changes, even at the edges of crystals, and (ii) the size of each crystallite is some tens of nanometers smaller than is the case with thermal polymerisation. The coherent crystal size is smaller in comparison with the thermal treatment, in which larger coherent crystals are formed at the final state of polymerisation, whereas the small domain structures are observed as the intermediate stage of thermal polymerisation. In the case of electron-induced polymerisation, we could not observe the coexistence of monomer and polymer regions, because this radiation polymerisation is so rapid that it is hard to stop the reaction at an intermediate stage. However, from the micro domain morphology (mosaic nature) observed at fully polymerised stage, many nuclei for polymerisation have been formed sporadically at the initial stage of polymerisation and continued to grow up to a small polymer domain, almost keeping topochemical relation.

In conclusion, the polymerisation processes by thermal treatment and electron irradiation can be sketched schematically in *Figure 10*. The needle-like crystal is represented by the large rectangular frame in the figure, where the monomer and polymer regions are indicated by different screen-tones. In the case of thermal polymerisation, the reaction is preferentially started 'heterogeneously' at an edge of the crystal where the volume can expand freely (the left figure of *Figure 10a*). Nearby the polymer region, there are small domains of transient state (mixed state of polymer and monomer). After further polymerisation, the polymerised regions extend inside the crystal through structural transient states. As polymerisation proceeds, the polymer crystals often change their orientation at the edges of the needle-like crystal, possibly due to relaxation of internal stresses produced by polymerisation. As a result, the polymer crystal exhibits a fibrous character. In contrast, in the case of electron irradiation polymerisation, the whole area is excited uniformly by electron irradiation and polymerisation is initiated 'homogeneously' at many points in the crystal (the left figure of *Figure 10b*). Subsequently, polymerisation proceeds from each polymerising nucleus, so that many small polymer crystallites are formed. The crystallites do not have a fibrous texture, but small spherical domains aggregate without any drastic changes in orientation. The internal stress produced by polymerisation may be relaxed by changing slightly the relative orientation of the crystallites in this case. In general, the polymer film produced by electron irradiation exhibits a homogeneous orientation.

ACKNOWLEDGEMENTS

This work was partly supported by a Grant-in-Aid for Scientific Research on Priority Area, the Ministry of Education, Science, Sports and Culture, Japan.

REFERENCES

1. Wegner, G., *Zeitschrift für Naturforschung, Teil B*, 1969, **24**, 824.
2. Baughman, R. H., *Journal of Applied Physics*, 1972, **43**, 4362.
3. Baughman, R. H., *Journal of Polymer Science, Polymer Physics Edition*, 1974, **12**, 1511.
4. Yee, K. C., *Journal of Polymer Science, Polymer Physics Edition*, 1978, **16**, 431.
5. Enkelmann, V. and Wegner, G., *Makromolekulare Chemie*, 1978, **180**, 1787.
6. Enkelmann, V., Wegner, G., Eichele, H. and Schwoerer, M., *Chemical Physics Letters*, 1977, **52**, 314.
7. Read, R. T. and Young, R. J., *Journal of Materials Science*, 1984, **19**, 327.
8. Yeung, P. H. J. and Young, R. Y., *Polymer*, 1986, **27**, 202.
9. Kobayashi, T. and Uyeda, N., *Journal of Crystal Growth* 1987, **84**, 589; *ibid.* 1990, **100**, 676.
10. Kobayashi, T. and Uyeda, N., *Philosophical Magazine*, 1988, **B57**, 493.
11. Tsuji, M., Isoda, S., Ohara, M., Kawaguchi, A. and Katayama, K., *Polymer*, 1982, **23**, 1568.
12. Isoda, S., Tsuji, M., Ohara, M., Kawaguchi, A. and Katayama, K., *Polymer*, 1983, **24**, 1155.
13. Kawase, N., Kubono, K., Isoda, S. and Kobayashi, T., *Journal of Polymer Science, Polymer Physics Edition*, 1993, **31**, 1713.
14. Liao, J. and Martin, D. C., *Science*, 1993, **260**, 1489.
15. Fujiyoshi, Y., Kobayashi, T., Ishizuka, K., Uyeda, N., Ishida, Y. and Harada, Y., *Ultramicroscopy*, 1980, **5**, 459.
16. Enkelmann, V., Leyrer, R. J., Schleier, G. and Wegner, G., *Journal of Materials Science*, 1980, **15**, 168.
17. Le Moigne, J., Thierry, A., Chollet, A., Kajzar, F. and Messier, J., *Journal of Chemical Physics*, 1988, **88**, 6647.
18. Apgar, P. A., *Acta Crystallographica*, 1978, **B34**, 957.
19. Enkelmann, V., Schleier, G. and Eichele, H., *Journal of Materials Science*, 1982, **17**, 533.